Commensurability and Finite Size Effects in Lattice Simulations of Diblock Copolymers

Akash Arora, David C. Morse, Frank S. Bates, and Kevin D. Dorfman

Department of Chemical Engineering and Materials Science, University of Minnesota–Twin Cities, 421 Washington Ave. SE, Minneapolis, Minnesota 55455, United States

Supporting Information

CONTENTS

I. Heat capacity evidence of a first-order phase transition 2

II. All Systems (commensurate and incommensurate) 2

III. Commensurate systems 4

IV. Tabulated Data for Commensurate Systems 7

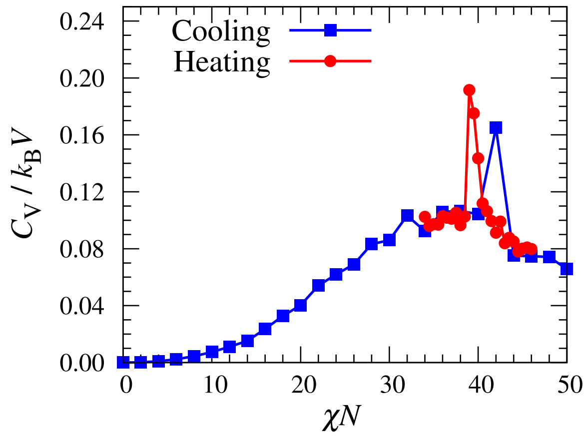

FIG. S-1. Heat capacity for both cooling (blue) and heating run (red) obtained at constant step size of $\Delta(\chi N) = 0.5$. The spike in the heat capacity correspond to the two ends of hysteresis loop presented in Fig. 1 in the main text.

I. HEAT CAPACITY EVIDENCE OF A FIRST-ORDER PHASE TRANSITION

Figure S-1 shows the heat capacity scaled with the number of sites is the system, $C_V/k_\mathrm{B}V$, for the complete heating run. The spike in the heat capacity corresponds to the discontinuity at the two ends of the hysteresis loop presented in the Fig. 1 of the main manuscript. The spike in the heat capacity is consistent with the presence of a first-order transition.

II. ALL SYSTEMS (COMMENSURATE AND INCOMMENSURATE)

In the main text, we claimed that the trends with respect to system size L are not systematic for arbitrary values of L. In this section of the supporting information, we provide data at regular spacing in L to support our claim with respect to the hysteresis loops, structure factor, and chain size metrics.

We begin with the hysteresis loop. Figure S-2 depicts the hysteresis loop obtained for the six systems in the range $L = 24$ to $L = 64$ with $\Delta L = 8$. The hysteresis loop for $L = 48$ begins quite early and has a significantly wide metastability region, while for $L = 64$, the hysteresis has moved to a high χN value. Moreover, for the smallest system considered, $L = 24$, the nucleation and melting of lamella is fast, resulting in a negligible supercooling

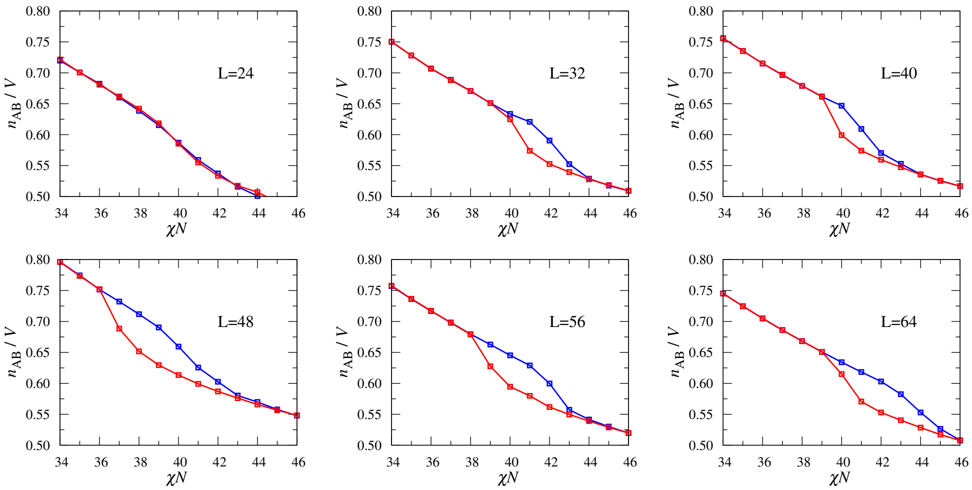

FIG. S-2. Number of AB contacts, n_{AB}/V, as a function of segregation strength, χN, for both cooling (blue) and heating (red) runs. The data correspond to the constant step size of $\Delta(\chi N) = 1.0$.

and superheating. It is clear from the figure that both the widths and positions of the hysteresis do not vary systematically with L.

Figure S-3 shows the evolution of the peak of the structure factor in the disordered phase. As the segregation strength χN increases, the peak in the structure factor varies non-monotonically with L. The peak for $L = 48$ is highest among all of the systems for the complete run, while peak for the largest system, $L = 64$, never becomes highest during the complete run.

Figure S-4 shows the radius of gyration, R_g^2, and the separation between the blocks' centers-of-mass, R_{AB}^2, as a function of segregation strength, χN. The chain dimension increases significantly as the system approaches toward the order-disorder transition (ODT) confirming the stretching of chains in the ordered phase. However, the increase in R_g^2 and R_{AB}^2 is not systematic with L. In the disordered phase ($\chi N < 40$), $L = 48$ has the maximum chain dimensions, while in the ordered phase the chain dimensions for $L = 32$ becomes maximum.

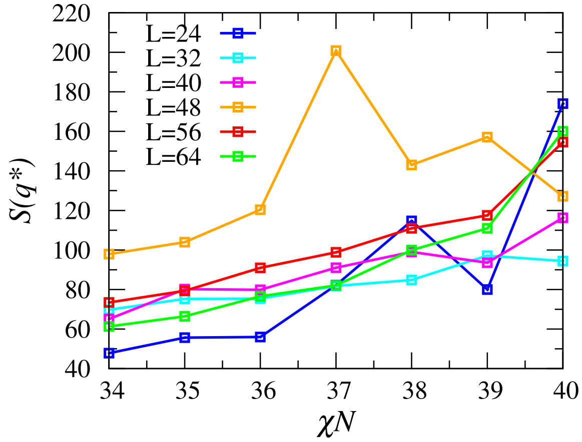

FIG. S-3. Peak of the structure factor, $S(q^*)$ against the segregation strength in the disordered phase. The results are calculated with a step size $\Delta(\chi N) = 1.0$.

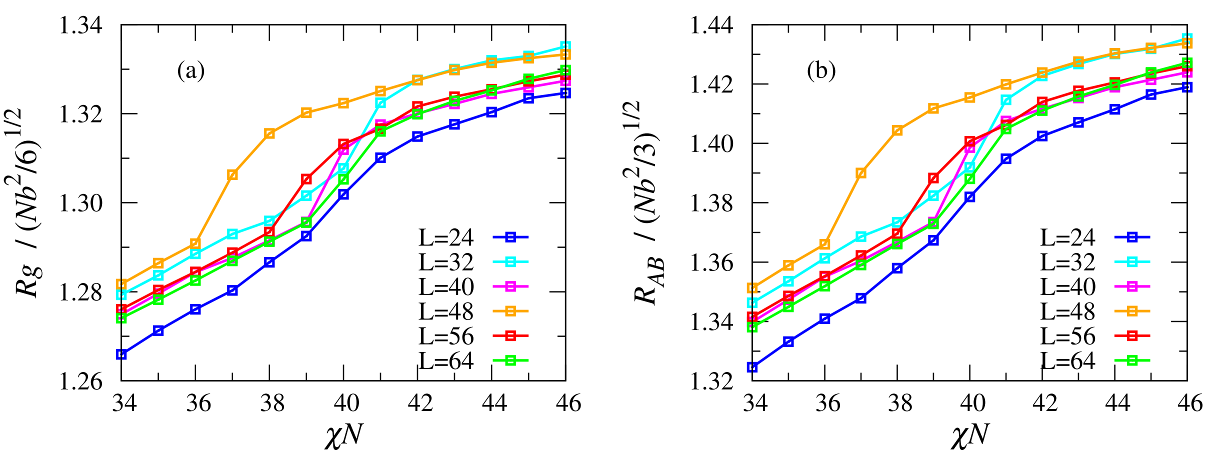

FIG. S-4. (a) Radius of gyration, R_g^2, (b) separation between the the blocks' centers-of-mass, R_{AB}^2, against the segregation strength for the complete cooling run. The results are calculated with a step size of $\Delta(\chi N) = 1.0$.

III. COMMENSURATE SYSTEMS

In the main text, we mentioned that (i) some of the commensurate systems do not necessarily form lamella in the principle lattice directions and (ii) metrics in addition to the structure factor show systematic behavior with respect to L when we only consider the commensurate systems. In this section, we provide data supporting these claims.

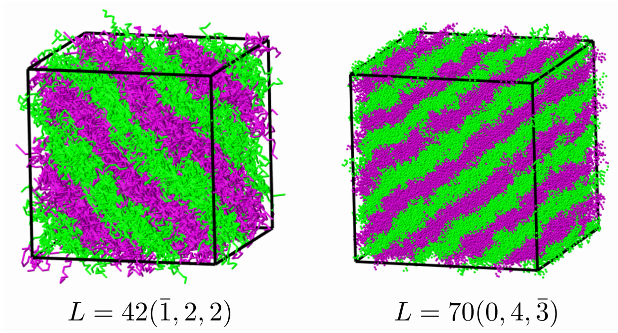

FIG. S-5. Snapshots of the lamellar configuration formed in the direction, (a) $(\bar{1}22)$ for $L = 42$, and (b) $(04\bar{3})$ for $L = 70$.

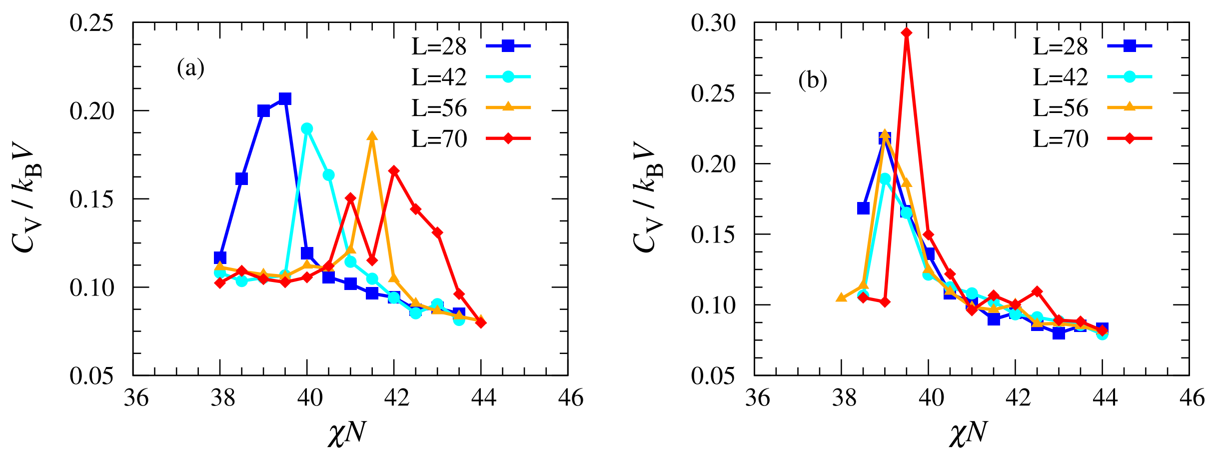

FIG. S-6. Heat capacity, C_V/k_BT against the segregation strength, χN, for (a) cooling run, and (b) heating run. The results are obtained for all four commensurate systems with a constant step size of $\Delta(\chi N) = 0.5$.

Figure S-5 shows the configuration of the lamellar phase formed in the directions $(\bar{1}22)$ and $(04\bar{3})$ for the system sizes $L = 42$ and $L = 70$, respectively. For both of the systems, out of eight statistical independent runs, half of the runs produce lamella along the principle directions while others produce lamella tilted with respect to principle direction, as shown in Fig. S-5.

Figure S-6 depicts the heat capacity for both cooling and heating runs for the four commensurate systems obtained by the approach described in the main text. The spike in the heat capacity confirms the presence of a fluctuation-driven, weakly first-order transition. Moreover, for the cooling run, the spike shifts towards higher segregation strength as the

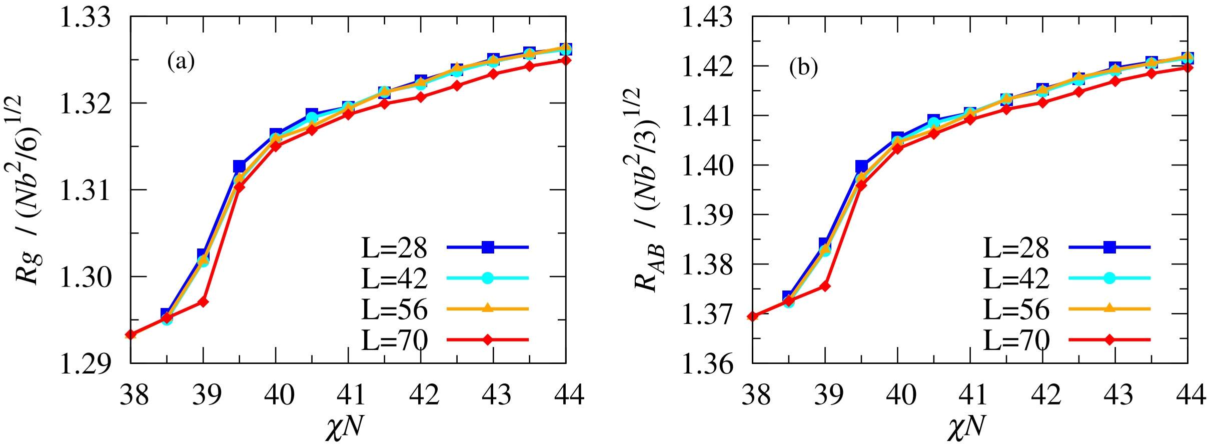

FIG. S-7. (a) Radius of gyration, R_g^2, (b) separation between the the blocks' centers-of-mass, R_{AB}^2 against the segregation strength for all the commensurate systems. The results are calculated for a constant step size of $\Delta(\chi N) = 0.5$.

system size L increases, while for the heating run the spike remains almost unaffected by the change in L. The shift for the cooling run demonstrates the increase in the degree of supercooling while the heating branch does not experience appreciable superheating. Therefore, the ODT lies very close to the heating branch. It is clear from Fig. S-6 that the ODT does not change with system size and finite size effects are not pronounced in the simulation model considered here.

Note that there are two peaks in the heat capacity for $L = 70$. We believe that it is an artifact that arises because the system repeatedly flips between the disordered phase and metastable ordered phase during the cooling run. This can result in significant variance in the internal energy and so first the spike occurs. However, maximum spike in the heat capacity should have occurred only when the system forms an equilibrium ordered phase undergoing a discontinuity at the right end of the hysteresis. Therefore, the second spike denotes the transition correctly and not the first spike.

Figure S-7 shows the chain dimensions, R_g^2 and R_{AB}^2, for the four commensurate systems. It is clear from the figure that all four systems have the same chain dimension, both in the ordered and the disordered phases. This demonstrates that the finite size effects do not affect the chain dimensions for commensurate conditions.

IV. TABULATED DATA FOR COMMENSURATE SYSTEMS

For completeness, we provide the tabulated data for all metrics near the ODT for commensurate systems in both heating and cooling runs.

TABLE I. $L = 28$: Cooling run

χN	R_g^2	R_{AB}^2	$\langle n_{AB}\rangle/V$	C_V/K_BT	$S(q^*)$
38.5	10.076 ± 0.116	24.535 ± 0.122	0.6619 ± 0.0231	0.1613 ± 0.0908	479
39.0	10.155 ± 0.129	24.822 ± 0.407	0.6436 ± 0.0240	0.1998 ± 0.0942	709
39.5	10.330 ± 0.078	25.436 ± 0.450	0.6071 ± 0.0142	0.2068 ± 0.1152	1325
40.0	10.400 ± 0.017	25.692 ± 0.274	0.5890 ± 0.0027	0.1192 ± 0.0197	1580
40.5	10.428 ± 0.022	25.791 ± 0.060	0.5810 ± 0.0024	0.1057 ± 0.0116	1637
41.0	10.453 ± 0.011	25.887 ± 0.041	0.5734 ± 0.0023	0.1018 ± 0.0090	1682
41.5	10.469 ± 0.022	25.946 ± 0.072	0.5670 ± 0.0022	0.0964 ± 0.0070	1721
42.0	10.485 ± 0.012	26.014 ± 0.042	0.5612 ± 0.0018	0.0943 ± 0.0065	1756
42.5	10.518 ± 0.013	26.134 ± 0.045	0.5534 ± 0.0019	0.0873 ± 0.0031	1814
43.0	10.526 ± 0.010	26.169 ± 0.038	0.5486 ± 0.0013	0.0883 ± 0.0082	1831
43.5	10.551 ± 0.016	26.257 ± 0.054	0.5428 ± 0.0018	0.0850 ± 0.0084	1869

TABLE II. $L = 28$: Heating run

χN	R_g^2	R_{AB}^2	$\langle n_{AB} \rangle / V$	$C_V / K_B T$	$S(q^*)$
38.5	10.073 ± 0.121	24.5224 ± 0.423	0.6613 ± 0.0236	0.1685 ± 0.0809	583
39.0	10.179 ± 0.113	24.9036 ± 0.398	0.6385 ± 0.0217	0.2178 ± 0.0961	572
39.5	10.339 ± 0.021	25.4700 ± 0.066	0.6044 ± 0.0031	0.1663 ± 0.0184	1478
40.0	10.397 ± 0.024	25.6790 ± 0.081	0.5909 ± 0.0038	0.1360 ± 0.0224	1530
40.5	10.434 ± 0.019	25.8080 ± 0.063	$0.5814 \pm 0..0037$	0.1080 ± 0.0200	1634
41.0	10.447 ± 0.019	25.8635 ± 0.061	0.5740 ± 0.0015	0.1013 ± 0.0259	1677
41.5	10.474 ± 0.023	25.9634 ± 0.079	0.5663 ± 0.0025	0.0897 ± 0.0142	1733
42.0	10.495 ± 0.013	26.0402 ± 0.045	0.5603 ± 0.0014	0.0943 ± 0.0297	1764
42.5	10.515 ± 0.007	26.1189 ± 0.025	0.5540 ± 0.0019	0.0857 ± 0.0055	1824
43.0	10.535 ± 0.001	26.1976 ± 0.048	0.5477 ± 0.0017	0.0799 ± 0.0085	1852
43.5	10.546 ± 0.003	26.2404 ± 0.040	0.5431 ± 0.0016	0.0850 ± 0.0055	1862

TABLE III. $L = 42$: Cooling run

χN	R_g^2	R_{AB}^2	$\langle n_{AB} \rangle / V$	$C_V / K_B T$	$S(q^*)$
38.5	10.067 ± 0.010	24.496 ± 0.034	0.6692 ± 0.0009	0.1035 ± 0.0056	177
39.0	10.104 ± 0.006	24.636 ± 0.022	0.6586 ± 0.0016	0.1054 ± 0.0104	245
39.5	10.131 ± 0.007	24.731 ± 0.025	0.6516 ± 0.0019	0.1067 ± 0.0053	261
40.0	10.207 ± 0.076	25.005 ± 0.270	0.6326 ± 0.0187	0.1898 ± 0.1362	1180
40.5	10.291 ± 0.105	25.309 ± 0.368	0.6109 ± 0.0230	0.1636 ± 0.0945	2347
41.0	10.386 ± 0.114	25.649 ± 0.401	0.5890 ± 0.0238	0.1144 ± 0.0288	3805
41.5	10.457 ± 0.063	25.907 ± 0.217	0.5677 ± 0.0072	0.1048 ± 0.0129	5233
42.0	10.490 ± 0.072	26.026 ± 0.244	0.5601 ± 0.0071	0.0940 ± 0.0088	5526
42.5	10.503 ± 0.070	26.079 ± 0.238	0.5541 ± 0.0067	0.0852 ± 0.0052	5690
43.0	10.528 ± 0.076	26.167 ± 0.257	0.5478 ± 0.0069	0.0904 ± 0.0051	5836
43.5	10.542 ± 0.070	26.224 ± 0.241	0.5421 ± 0.0071	0.0814 ± 0.0064	5960

TABLE IV. $L = 42$: Heating run

χN	R_g^2	R_{AB}^2	$\langle n_{AB} \rangle / V$	$C_V / K_B T$	$S(q^*)$
38.5	10.063 ± 0.012	24.482 ± 0.037	0.6695 ± 0.0013	0.1065 ± 0.0090	184
39.0	10.167 ± 0.066	24.854 ± 0.231	0.6456 ± 0.0143	0.1892 ± 0.0730	1216
39.5	10.313 ± 0.064	25.374 ± 0.222	0.6108 ± 0.0140	0.1651 ± 0.0138	3408
40.0	10.390 ± 0.023	25.650 ± 0.078	0.5918 ± 0.0024	0.1214 ± 0.0071	4509
40.5	10.427 ± 0.016	25.789 ± 0.056	0.5814 ± 0.0025	0.1124 ± 0.0376	4981
41.0	10.447 ± 0.008	25.861 ± 0.029	0.5741 ± 0.0013	0.1081 ± 0.0117	5106
41.5	10.475 ± 0.012	25.967 ± 0.040	0.5664 ± 0.0016	0.1023 ± 0.0092	5358
42.0	10.488 ± 0.009	26.022 ± 0.030	0.5604 ± 0.0008	0.0933 ± 0.0080	5496
42.5	10.513 ± 0.006	26.110 ± 0.020	0.5539 ± 0.0004	0.0912 ± 0.0055	5658
43.0	10.530 ± 0.010	26.176 ± 0.035	0.5485 ± 0.0013	0.0884 ± 0.0066	5798
43.5	10.544 ± 0.008	26.231 ± 0.026	0.5427 ± 0.0007	0.0857 ± 0.0035	5942

TABLE V. $L = 56$: Cooling run

χN	R_g^2	R_{AB}^2	$\langle n_{AB} \rangle / V$	$C_V / K_B T$	$S(q^*)$
38.5	10.064 ± 0.006	24.488 ± 0.019	0.6710 ± 0.0005	0.1089 ± 0.0105	212
39.0	10.096 ± 0.006	24.605 ± 0.020	0.6617 ± 0.0011	0.1072 ± 0.0147	232
39.5	10.127 ± 0.007	24.718 ± 0.026	0.6538 ± 0.0009	0.1061 ± 0.0074	285
40.0	10.160 ± 0.009	24.838 ± 0.033	0.6450 ± 0.0020	0.1123 ± 0.0224	430
40.5	10.191 ± 0.009	24.953 ± 0.030	0.6366 ± 0.0015	0.1106 ± 0.0073	400
41.0	10.228 ± 0.019	25.091 ± 0.067	0.6275 ± 0.0043	0.1208 ± 0.0430	667
41.5	10.350 ± 0.087	25.529 ± 0.305	0.5932 ± 0.0217	0.1850 ± 0.1435	5459
42.0	10.478 ± 0.037	25.986 ± 0.125	0.5622 ± 0.0033	0.1046 ± 0.0225	12199
42.5	10.500 ± 0.041	26.069 ± 0.139	0.5558 ± 0.0034	0.0907 ± 0.0050	13170
43.0	10.515 ± 0.038	26.125 ± 0.129	0.5501 ± 0.0030	0.0864 ± 0.0060	12845
43.5	10.531 ± 0.042	26.187 ± 0.144	0.5442 ± 0.0035	0.0835 ± 0.0063	13450

TABLE VI. $L = 56$: Heating run

χN	R_g^2	R_{AB}^2	$\langle n_{AB}\rangle/V$	C_V/K_BT	$S(q^*)$
38.5	10.066 ± 0.006	24.494 ± 0.021	0.6706 ± 0.0009	0.1135 ± 0.0212	233
39.0	10.169 ± 0.092	24.860 ± 0.323	0.6456 ± 0.0196	0.2202 ± 0.1837	2780
39.5	10.317 ± 0.030	25.388 ± 0.105	0.6103 ± 0.0055	0.1856 ± 0.0696	7186
40.0	10.389 ± 0.007	25.647 ± 0.024	0.5925 ± 0.0007	0.1247 ± 0.0153	9496
40.5	10.412 ± 0.010	25.735 ± 0.033	0.5839 ± 0.0009	0.1093 ± 0.0172	10338
41.0	10.444 ± 0.006	25.855 ± 0.019	0.5753 ± 0.0008	0.0984 ± 0.0077	10926
41.5	10.474 ± 0.013	25.964 ± 0.043	0.5677 ± 0.0013	0.0965 ± 0.0035	11902
42.0	10.491 ± 0.008	26.029 ± 0.027	0.5615 ± 0.0008	0.1004 ± 0.0090	12059
42.5	10.518 ± 0.008	26.129 ± 0.028	0.5543 ± 0.0006	0.0864 ± 0.0033	12982
43.0	10.532 ± 0.010	26.184 ± 0.032	0.5488 ± 0.0005	0.0868 ± 0.0052	13093
43.5	10.543 ± 0.005	26.232 ± 0.033	0.5433 ± 0.0008	0.0849 ± 0.0056	13282

TABLE VII. $L = 70$: Cooling run

χN	R_g^2	R_{AB}^2	$\langle n_{AB}\rangle/V$	C_V/K_BT	$S(q^*)$
38.5	10.065 ± 0.005	24.488 ± 0.017	0.6684 ± 0.0008	0.1092 ± 0.0129	210
39.0	10.101 ± 0.007	24.619 ± 0.024	0.6595 ± 0.0008	0.1046 ± 0.0075	240
39.5	10.133 ± 0.007	24.737 ± 0.025	0.6509 ± 0.0010	0.1028 ± 0.0079	244
40.0	10.157 ± 0.004	24.826 ± 0.014	0.6435 ± 0.0006	0.1056 ± 0.0104	249
40.5	10.191 ± 0.005	24.951 ± 0.018	0.6347 ± 0.0005	0.112 ± 0.0120	374
41.0	10.227 ± 0.014	25.082 ± 0.050	0.6256 ± 0.0037	0.1505 ± 0.0885	1145
41.5	10.274 ± 0.062	25.253 ± 0.221	0.6134 ± 0.0170	0.1152 ± 0.0164	3624
42.0	10.336 ± 0.073	25.478 ± 0.261	0.5960 ± 0.0197	0.1659 ± 0.0832	8400
42.5	10.413 ± 0.065	25.759 ± 0.232	0.5721 ± 0.0188	0.1442 ± 0.0674	12895
43.0	10.468 ± 0.035	25.961 ± 0.123	0.5545 ± 0.0068	0.131 ± 0.1016	20138
43.5	10.490 ± 0.037	26.045 ± 0.130	0.5471 ± 0.0065	0.0961 ± 0.0045	22166

TABLE VIII. $L = 70$: Heating run

χN	R_g^2	R_{AB}^2	$\langle n_{AB} \rangle / V$	$C_V / K_B T$	$S(q^*)$
38.5	10.098 ± 0.006	24.607 ± 0.021	0.6599 ± 0.0004	0.1021 ± 0.0075	178
39.0	10.266 ± 0.003	25.207 ± 0.012	0.6174 ± 0.0004	0.2926 ± 0.0124	221
39.5	10.355 ± 0.050	25.524 ± 0.173	0.5943 ± 0.0107	0.1498 ± 0.1319	11755
40.0	10.393 ± 0.036	25.667 ± 0.125	0.5824 ± 0.0071	0.1218 ± 0.0241	17738
40.5	10.420 ± 0.033	25.770 ± 0.115	0.5735 ± 0.0052	0.0961 ± 0.0160	20931
41.0	10.439 ± 0.027	25.839 ± 0.091	0.5673 ± 0.0041	0.1067 ± 0.0090	21968
41.5	10.455 ± 0.029	25.906 ± 0.100	0.5609 ± 0.0050	0.1001 ± 0.0096	22265
42.0	10.472 ± 0.025	25.969 ± 0.086	0.5550 ± 0.0044	0.1095 ± 0.0129	22241
42.5	10.478 ± 0.029	25.999 ± 0.100	0.5505 ± 0.0046	0.0891 ± 0.0270	23961
43.0	10.492 ± 0.021	26.051 ± 0.073	0.5455 ± 0.0036	0.0882 ± 0.0077	26012
43.5	10.495 ± 0.026	26.070 ± 0.090	0.5422 ± 0.0040	0.0817 ± 0.0059	25745